PHYSICAL REVIEW D, VOLUME 62, 055014

Constraints on two-Higgs-doublet models at large tan β from W and Z decays

Oleg Lebedev,* Will Loinaz,† and Tatsu Takeuchi‡
Physics Department, Institute for Particle Physics and Astrophysics, Virginia Tech, Blacksburg, Virginia 24061
(Received 10 February 2000; published 11 August 2000)

We study constraints on type-II two-Higgs-doublet models at large tan β from CERN LEP and SLD Z-pole data and from lepton universality violation in W decay. We perform a global fit and find that, in the context of Z decay, the LEP–SLD experimental values for lepton universality violation, R_b, and A_b all somewhat disfavor the model. Contributions from the neutral-Higgs sector can be used to constrain the scalar–pseudoscalar Higgs mass splittings. Contributions from the charged-Higgs sector allow us to constrain the charged-Higgs boson mass. For $\tan\beta=100$ we obtain the 1σ classical (Bayesian) bounds of $m_{H^\pm} \geqslant 670\,\mathrm{GeV}$ (370 GeV) and $1 \geqslant m_{h^0}/m_{A^0}|_{\alpha=\beta} = m_{H^0}/m_{A^0}|_{\alpha=0} \geqslant 0.68$ (0.64). The 2σ bounds are weak. Currently, the Fermilab Tevatron experimental limits on lepton universality violation in W decay provide no significant constraint on the Higgs sector.

PACS number(s): 12.60.Fr, 12.15.Lk, 13.38.Be, 13.38.Dg

I. INTRODUCTION

Perhaps the most important unanswered question in particle physics today is ''What is the nature of electroweak symmetry breaking?'' The standard model (SM) incorporates the simplest mechanism: a Higgs sector consisting of a single self-interacting scalar SU(2) doublet of hypercharge $Y=1$. Upon breaking of electroweak symmetry, the physical spectrum of the SM Higgs sector consists of one CP-even neutral Higgs particle. Current experimental data do not definitively contradict the SM, but persistent deviations in precision electroweak data from SM predictions on the edge of statistical significance tantalize us with the possibility of new physics. This, together with various theoretical prejudices which suggest that the SM cannot be a complete theory, motivates the detailed study of alternative scenarios of eletroweak symmetry breaking (EWSB).

The two-Higgs-doublet model (2HDM) [1] is the most straightforward extension of the EWSB mechanism of the SM. The theory proposes a pair of scalar SU(2) doublets, both with hypercharge $Y=1$. Depending on the version of the 2HDM, these scalars may couple in various ways to the quarks and leptons. After electroweak symmetry is broken, the spectrum of the Higgs sector consists of five physical Higgs bosons: two neutral CP-even scalars (h_0 and H_0), a neutral CP-odd scalar (A_0), and a pair of charged scalars ($H^\pm$). These particles could be detected via direct production at colliders, but their effects may also be visible indirectly, through their contributions as intermediate states in decay processes.

In this paper we consider the indirect signatures of the 2HDM in flavor-conserving W and Z decays through its contribution to decay amplitudes via loop corrections. We consider only type-II 2HDM models, in which the $I_3=\frac{1}{2}$ fermions couple to one Higgs doublet and the $I_3=-\frac{1}{2}$ fermions couple to the other. We also focus on the large tan β region,[1] in which the Higgs couplings to the down-type quarks and the charged leptons are enhanced.[2] This can potentially lead to observable (or constrainable) flavor-dependent corrections in Z and W decay, especially for the third generation (b and τ). Additional strong constraints on the charged-Higgs boson mass ($\geqslant$380 GeV) are available from $b\to s\gamma$ (see, for example, Refs. [3,4]).

One-loop corrections to flavor-conserving Z decays in the 2HDM have been considered previously in Refs. [5–9], including as a possible explanation for the now-defunct ''R_b anomaly.'' The Z-pole runs at the CERN e^+e^- collider LEP and SLAC Large Detector (SLD) are complete and essentially all of the data have been analyzed. The ''R_b anomaly'' has disappeared only to be replaced by the ''A_b anomaly'' [10,11]; thus, it is timely to revisit the model. We perform, for the first time, a global fit to all LEP–SLD Z-pole observables, and we examine the competing constraints from lepton universality, R_b, and A_b on the charged and neutral sectors of the model. In addition, we study constraints on the model from lepton universality violation in W decays, which have not been previously considered.

II. LEPTONIC W DECAYS

In this section we calculate the constraints on the large-tan β 2HDM from lepton universality violation in W decays. We use the Feynman rules and conventions of Ref. [12]. Our notation for the scalar and tensor integrals is established in Ref. [13].

*Email address: lebedev@quasar.phys.vt.edu
†Email address: loinaz@alumni.princeton.edu
‡Email address: takeuchi@vt.edu

[1]Perturbativity of the b and t Yukawa couplings requires $0.3 \leqslant \tan\beta \leqslant 120$ (see, for example [1]).

[2]This model is often studied embedded in the minimal supersymmetric extension of the standard model (MSSM) [2], although we do not consider it in this context here.

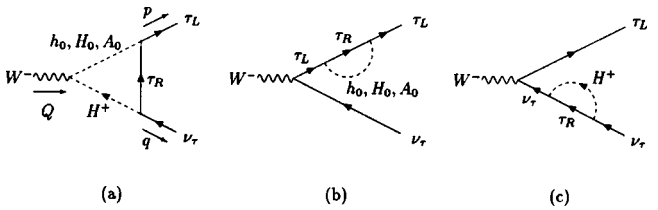

FIG. 1. One-loop corrections to $W^- \to \tau_L \overline{\nu}_\tau$.

The leading (in $\tan\beta$) one-loop corrections to the decay $W^- \to \tau^- \overline{\upsilon}_\tau$ are shown in Fig. 1. The corresponding contributions to the amplitude are[3]

$$
\begin{aligned}
&-\frac{g^2}{4}\left(\frac{m_\tau \tan\beta}{m_W}\right)^2\left[-i\frac{g}{\sqrt{2}}W^\mu(Q)\overline{\tau}(p)\gamma_\mu P_L \nu_\tau(q)\right] \\
&\quad\times(1a/h^0):\sin^2\alpha\ 2\hat{C}_{24}(0,0,Q^2;0,m_{h^0},m_{H^\pm}) \\
&\quad\times(1a/H^0):\cos^2\alpha\ 2\hat{C}_{24}(0,0,Q^2;0,m_{H^0},m_{H^\pm}) \\
&\quad\times(1a/A^0):2\hat{C}_{24}(0,0,Q^2;0,m_{A^0},m_{H^\pm}) \\
&\quad\times(1b/h^0):\sin^2\alpha\ B_1(0;0,m_{h^0}) \\
&\quad\times(1b/H^0):\cos^2\alpha\ B_1(0;0,m_{H^0}) \\
&\quad\times(1b/A^0):B_1(0;0,m_{A^0}) \\
&\quad\times(1c):2B_1(0;0,m_{H^\pm})
\end{aligned}
\tag{2.1}
$$

with $Q^2=m_W^2$. The tree level amplitude is the expression in the square brackets. For the diagrams involving h^0 and H^0, we have dropped terms subleading in $\tan\beta$.[4] In the above we have made the large $\tan\beta$ approximations:

$$
\begin{aligned}
\cos(\beta-\alpha)&\approx\sin\alpha, \\
\sin(\beta-\alpha)&\approx\cos\alpha, \\
\sin\beta&\approx 1, \\
\cos\beta&\approx 0.
\end{aligned}
\tag{2.2}
$$

Combining the above corrections, with factors of 1/2 for the wave-function renormalization diagrams (1b) and (1c), leads to a shift in the $W\tau\overline{\nu}_\tau$ coupling given by

$$
\begin{aligned}
\frac{\delta g_\tau}{g}=&-\frac{g^2}{2}\left(\frac{m_\tau\tan\beta}{m_W}\right)^2[\sin^2\alpha\{\hat{C}_{24}(0,m_{h^0},m_{H^\pm}) \\
&+\tfrac{1}{4}B_1(0,m_{h^0})+\tfrac{1}{4}B_1(0,m_{H^\pm})\} \\
&+\cos^2\alpha\{\hat{C}_{24}(0,m_{H^0},m_{H^\pm})+\tfrac{1}{4}B_1(0,m_{H^0}) \\
&+\tfrac{1}{4}B_1(0,m_{H^\pm})\}+\{\hat{C}_{24}(0,m_{A^0},m_{H^\pm})+\tfrac{1}{4}B_1(0,m_{A^0}) \\
&+\tfrac{1}{4}B_1(0,m_{H^\pm})\}],
\end{aligned}
\tag{2.3}
$$

where we have suppressed the external momentum dependence of the integrals for notational simplicity. Similar shifts to the $W\mu\overline{\nu}_\mu$ and $We\overline{\nu}_e$ vertices exist but they are suppressed by factors of $(m_\mu/m_\tau)^2$ and $(m_e/m_\tau)^2$ so we neglect them.

The complete expression for the finite combination of integrals seen in the curly brackets of Eq. (2.3), namely,

$$
\begin{aligned}
\zeta(Q^2;m_1,m_2)\equiv&\hat{C}_{24}(0,0,Q^2;0,m_1,m_2)+\tfrac{1}{4}B_1(0;0,m_1) \\
&+\tfrac{1}{4}B_1(0;0,m_2),
\end{aligned}
\tag{2.4}
$$

can be found in the appendix of Ref. [13]. However, for our purposes it will suffice to expand it in powers of $Q^2=m_W^2$:

$$
\begin{aligned}
\zeta(m_W^2;m_1,m_2)=&-\frac{1}{(4\pi)^2}\frac{1}{4}G\left(\frac{m_1^2}{m_2^2}\right) \\
&-\frac{1}{(4\pi)^2}\frac{m_W^2}{12(m_1^2-m_2^2)^2}\left[m_1^2+m_2^2\right. \\
&\left.-\frac{2m_1^2m_2^2}{m_1^2-m_2^2}\ln\frac{m_1^2}{m_2^2}\right]+\cdots,
\end{aligned}
\tag{2.5}
$$

where

$$
G(x)\equiv 1+\frac{1}{2}\left(\frac{1+x}{1-x}\right)\ln x. \tag{2.6}
$$

Observe that the function $G(x)$ is negative semidefinite so that the leading term is non-negative for all masses m_1 and m_2. This term dominates the subleading term unless the splitting between m_1 and m_2 is less than about $m_W/2$. In the limit that the masses are degenerate, the leading term vanishes and the expansion reduces to

$$
\zeta(m_W^2;m,m)=-\frac{1}{(4\pi)^2}\frac{m_W^2}{36m^2}+\cdots. \tag{2.7}
$$

In the limit $m_1\to\infty$ (the full expression is symmetric in m_1 and m_2) the expression becomes

$$
\zeta(m_W^2;m_1,m_2)\Rightarrow-\frac{1}{(4\pi)^2}\frac{1}{4}\left(1+\frac{1}{2}\ln\frac{m_2^2}{m_1^2}\right)+\cdots. \tag{2.8}
$$

Thus, Eq. (2.3) appears to lead to nondecoupling of heavy particles. That is, when m_{A^0} and $m_{H^\pm}$ are taken to be large independently, the amplitude does not vanish. However, in

[3]In computing the one-loop vertex corrections in both W and Z decays, it is a good approximation to neglect light fermion masses in loops.

[4]The subleading contributions of the h^0 and H^0 diagrams combine with the diagrams involving the Goldstone bosons to give finite results.

the general 2HDM the mass eigenvalues and mixing angle are related in such a way that if $m_{A^0}\to\infty$ while the couplings and the W mass are held fixed, the Higgs boson masses and mixing angle approach the limit [1]:

$$m_{H^0}\simeq m_{H^\pm}\simeq m_{A^0},\quad m_{h^0}/m_{A^0}\to 0,\quad \cos(\alpha-\beta)\to 0. \tag{2.9}$$

In this limit the amplitude vanishes and decoupling is obtained. This decoupling behavior can be understood as follows: In the large $\tan\beta$ limit, $\sin\alpha\to 0$ and the two Higgs doublets do not mix. Since large $\tan\beta$ implies $v_1\to 0$, electroweak symmetry is unbroken in the Φ_1 sector. The leading $\tan^2\beta$ diagrams are then due to the $W^-\Phi_1^{-*}\Phi_1^0$ vertex and corresponding wave-function renormalization diagrams (i.e., with Φ_1^0 and Φ_1^- in the loop). The sum of these diagrams vanishes at $p^2=0$ as a consequence of the Ward identity, and thus the heavy Higgs bosons decouple.[5]

Setting $m_{A^0}=m_{H^0}=m_{H^\pm}\equiv m$ and neglecting the m_{h^0} contribution, the shift in the coupling, Eq. (2.3), is small and positive:

$$\begin{aligned}\frac{\delta g_\tau}{g} &= -\frac{g^2}{2}\left(\frac{m_\tau\tan\beta}{m_W}\right)^2 2\zeta(m_W^2;m,m)\\ &\approx -\frac{g^2}{2}\left(\frac{m_\tau\tan\beta}{m_W}\right)^2\left\{-\frac{1}{(4\pi)^2}\frac{m_W^2}{18m^2}\right\}\\ &= \left(\frac{g m_\tau\tan\beta}{24\pi m}\right)^2.\end{aligned} \tag{2.10}$$

Away from this limit, the shift in the coupling is negative:

$$\begin{aligned}\frac{\delta g_\tau}{g} = \frac{1}{(4\pi)^2}\frac{g^2}{8}\left(\frac{m_\tau\tan\beta}{m_W}\right)^2\Bigg[&\sin^2\alpha\, G\left(\frac{m_{H^\pm}^2}{m_{h^0}^2}\right)\\ &+\cos^2\alpha\, G\left(\frac{m_{H^\pm}^2}{m_{H^0}^2}\right)+G\left(\frac{m_{H^\pm}^2}{m_{A^0}^2}\right)\Bigg]\leqslant 0.\end{aligned} \tag{2.11}$$

So, the model predicts a negative δg_τ, except in the limit that the Higgs mass splittings are small ($\leqslant m_W/2$). The magnitude of the shift is maximal for an extreme nondecoupling case in which the charged Higgs boson is much heavier than the neutral Higgs bosons. In this case it reduces to

$$\frac{\delta g_\tau}{g} = \frac{1}{(4\pi)^2}\frac{g^2}{4}\left(\frac{m_\tau\tan\beta}{m_W}\right)^2 G\left(\frac{m_{H^\pm}^2}{m_0^2}\right) \tag{2.12}$$

if we assign a common mass, m_0, to the neutral Higgs bosons.

The current bound on lepton universality violation in leptonic W decays from the DØ collaboration is [14]

$$\frac{g_\tau}{g_e} = 1.004\pm 0.019(\text{stat})\pm 0.026(\text{syst}). \tag{2.13}$$

The central value of δg_τ is positive, which is not allowed when the leading $G(x)$ term dominates. However, this fact is inconclusive since the experimental error is large. Using $\overline{m}_\tau(m_W)=1.777$ GeV and $2m_W/g=v=246$ GeV, and adding systematic and statistical errors in quadrature, we obtain from Eqs. (2.12) and (2.13):

$$G\left(\frac{m_{H^\pm}^2}{m_0^2}\right)=\left(\frac{100}{\tan\beta}\right)^2[1.2\pm 9.7]. \tag{2.14}$$

Since $G(x)$ negative semidefinite and invariant under $x\leftrightarrow 1/x$, at $\tan\beta=100$ this leads to a 1σ bound of

$$G\left(\frac{m_{H^\pm}^2}{m_0^2}\right)>-8.5$$

which translates to

$$\frac{m_0}{m_{H^\pm}}\quad\text{or}\quad\frac{m_{H^\pm}}{m_0}<1.3\times 10^4.$$

For smaller $\tan\beta$ the bound is even weaker.

Similarly, if we assume the limit of Eq. (2.10), the best-fit value of the common mass is (in GeV)

$$\left(\frac{100\,\text{GeV}}{m}\right)^2=\left(\frac{100}{\tan\beta}\right)^2[17\pm 132]. \tag{2.15}$$

At 1σ and $\tan\beta=100$, this translates into

$$m>8\ \text{GeV}$$

so, the bound is extremely weak in this mass-degenerate limit as well. Thus, even for $\tan\beta=100$ the current data gives no significant 1σ constraint on the Higgs boson masses.

III. CONSTRAINTS FROM LEP–SLD OBSERVABLES

In this section we perform a global analysis of LEP–SLD precision electroweak data in the context of the large $\tan\beta$ 2 HDM. We calculate the linearized shifts in the $Zf\overline{f}$ couplings from SM predictions, fit these shifts to the data, and use the results of the fit to constrain model parameters.

A. Corrections to the couplings

As in the W decay case, large $\tan\beta$ enhances the coupling of the Higgs sector to charged leptons and down-type quarks, but even then one only needs to consider the third generation fermions. Below we list corrections to $Z\to b\overline{b},\tau\overline{\tau},\nu_\tau\overline{\nu}_\tau$.

[5]The leading $\tan\beta$ contribution of the h^0 boson does not exhibit decoupling by itself: it is proportional to $\tan^2\beta\sin^2\alpha\ln m_{A^0}^2\to\ln m_{A^0}^2$ since $\sin\alpha\sim-\cos\beta+\mathcal{O}(m_Z^2/m_{A^0}^2)$ in the decoupling limit [1]. As the result is independent of $\tan\beta$, subleading $\tan\beta$ diagrams must be included to obtain the decoupling behavior.

The leading $\tan\beta$ corrections to the $Z\to b_R\bar{b}_R$ are shown in Figs. 2 and 3. The amplitudes of these diagrams are

$$
\begin{aligned}
&-\frac{g^2}{4}\left(\frac{m_b\tan\beta}{m_W}\right)^2\left[-i\frac{g}{\cos\theta_W}Z^\mu(Q)\bar{b}_R(p)\gamma_\mu b_R(q)\right]\\
&\quad\times(2a+2b/h^0):\sin^2\alpha\ 2\hat{C}_{24}(0,0,Q^2;0,m_{h^0},m_{A^0})\\
&\quad\times(2a+2b/H^0):\cos^2\alpha\ 2\hat{C}_{24}(0,0,Q^2;0,m_{H^0},m_{A^0})\\
&\quad\times(2c/h^0):h_{b_L}\sin^2\alpha\{(d-2)\hat{C}_{24}(0,0,Q^2;m_{h^0},0,0)-Q^2\hat{C}_{23}(0,0,Q^2;m_{h^0},0,0)\}\\
&\quad\times(2c/H^0):h_{b_L}\cos^2\alpha\{(d-2)\hat{C}_{24}(0,0,Q^2;m_{H^0},0,0)-Q^2\hat{C}_{23}(0,0,Q^2;m_{H^0},0,0)\}\\
&\quad\times(2c/A^0):h_{b_L}\{(d-2)\hat{C}_{24}(0,0,Q^2;m_{A^0},0,0)-Q^2\hat{C}_{23}(0,0,Q^2;m_{A^0},0,0)\}\\
&\quad\times(2d+2e/h^0):2h_{b_R}\sin^2\alpha\ B_1(0;0,m_{h^0})\\
&\quad\times(2d+2e/H^0):2h_{b_R}\cos^2\alpha\ B_1(0;0,m_{H^0})\\
&\quad\times(2d+2e/A^0):2h_{b_R}B_1(0;0,m_{A^0})\\
&\quad\times(3a):-4h_{H^+}\hat{C}_{24}(0,0,Q^2;m_t,m_{H^\pm},m_{H^\pm})\\
&\quad\times(3b):2h_{t_L}\{(d-2)\hat{C}_{24}(0,0,Q^2;m_{H^\pm},m_t,m_t)-Q^2\hat{C}_{23}(0,0,Q^2;m_{H^\pm},m_t,m_t)\}\\
&\quad\times(3c):-2h_{t_R}m_t^2\hat{C}_0(0,0,Q^2;m_{H^\pm},m_t,m_t)(3d+3e):4h_{b_R}B_1(0;m_t,m_{H^\pm}),
\end{aligned}
\tag{3.1}
$$

where

$$
h_f=I_{3f}-Q_f\sin^2\theta_W \tag{3.2}
$$

and $Q^2=m_Z^2$. The tree-level amplitude is the expression in the square brackets times h_{b_R}. As before, we have dropped terms subleading in $\tan\beta$. Combining these corrections, with factors of 1/2 for the wave-function renormalizations, leads to a shift in the right-handed coupling of the b to the Z given by

$$
\delta h_{b_R}=\delta h_{b_R}^N+\delta h_{b_R}^C, \tag{3.3}
$$

where

$$
\begin{aligned}
\delta h_{b_R}^N=&-\frac{g^2}{4}\left(\frac{m_b\tan\beta}{m_W}\right)^2[\sin^2\alpha\{2\hat{C}_{24}(0,m_{h^0},m_{A^0})+\tfrac{1}{2}B_1(0,m_{h^0})+\tfrac{1}{2}B_1(0,m_{A^0})\}\\
&+\cos^2\alpha\{2\hat{C}_{24}(0,m_{H^0},m_{A^0})+\tfrac{1}{2}B_1(0,m_{H^0})+\tfrac{1}{2}B_1(0,m_{A^0})\}+h_{b_L}\sin^2\alpha\{(d-2)\hat{C}_{24}(m_{h^0},0,0)\\
&-m_Z^2\hat{C}_{23}(m_{h^0},0,0)+B_1(0,m_{h^0})\}+h_{b_L}\cos^2\alpha\{(d-2)\hat{C}_{24}(m_{H^0},0,0)-m_Z^2\hat{C}_{23}(m_{H^0},0,0)+B_1(0,m_{H^0})\}\\
&+h_{b_L}\{(d-2)\hat{C}_{24}(m_{A^0},0,0)-m_Z^2\hat{C}_{23}(m_{H^0},0,0)+B_1(0,m_{A^0})\}],
\end{aligned}
$$

$$
\begin{aligned}
\delta h_{b_R}^C=&-\frac{g^2}{2}\left(\frac{m_b\tan\beta}{m_W}\right)^2[-h_{H^+}\{2\hat{C}_{24}(m_t,m_{H^\pm},m_{H^\pm})+B_1(m_t,m_{H^\pm})\}+h_{t_L}\{(d-2)\hat{C}_{24}(m_{H^\pm},m_t,m_t)\\
&-m_Z^2\hat{C}_{23}(m_{H^\pm},m_t,m_t)+B_1(m_t,m_{H^\pm})\}-h_{t_R}m_t^2\hat{C}_0(m_{H^\pm},m_t,m_t)].
\end{aligned}
\tag{3.4}
$$

As in the W decay case, these expressions can be well approximated by their leading terms in an expansion in m_Z^2 as long as the mass splittings among the Higgs bosons are not small.[6] Using the formulas from the preceding section and from the Appendix, we find

[6]Oblique corrections in the 2HDM with a *light* Higgs boson, i.e., large mass splittings, were recently considered in [15].

$$\delta h_{b_R}^N \approx + \frac{1}{(4\pi)^2}\frac{g^2}{8}\left(\frac{m_b \tan\beta}{m_W}\right)^2\left[\sin^2\alpha\ G\left(\frac{m_{h^0}^2}{m_{A^0}^2}\right)+\cos^2\alpha\ G\left(\frac{m_{H^0}^2}{m_{A^0}^2}\right)\right],$$

$$\delta h_{b_R}^C \approx + \frac{1}{(4\pi)^2}\frac{g^2}{4}\left(\frac{m_b \tan\beta}{m_W}\right)^2 F\left(\frac{m_t^2}{m_{H^\pm}^2}\right), \tag{3.5}$$

where the function $G(x)$ was defined in Eq. (2.6) and

$$F(x)=\frac{x}{1-x}\left(1+\frac{1}{1-x}\ln x\right). \tag{3.6}$$

See the Appendix for details.

The diagrams which correct the decay $Z\to b_L\overline{b_L}$ is the same as those shown in Figs. 2 and 3 with the replacements $b_R\leftrightarrow b_L$ and $t_L\leftrightarrow t_R$. The amplitudes of the neutral-Higgs diagrams are

$$\begin{aligned}
&+\frac{g^2}{4}\left(\frac{m_b\tan\beta}{m_W}\right)^2\left[-i\frac{g}{\cos\theta_W}Z^\mu(Q)\overline{b_L}(p)\gamma_\mu b_L(q)\right]\\
&\quad\times(2a+2b/h^0):\sin^2\alpha\ 2\hat{C}_{24}(0,0,Q^2;0,m_{h^0},m_{A^0})\\
&\quad\times(2a+2b/H^0):\cos^2\alpha\ 2\hat{C}_{24}(0,0,Q^2;0,m_{H^0},m_{A^0})\\
&\quad\times(2c/h^0):-h_{b_R}\sin^2\alpha\{(d-2)\hat{C}_{24}(0,0,Q^2;m_{h^0},0,0)-Q^2\hat{C}_{23}(0,0,Q^2;m_{h^0},0,0)\}\\
&\quad\times(2c/H^0):-h_{b_R}\cos^2\alpha\{(d-2)\hat{C}_{24}(0,0,Q^2;m_{H^0},0,0)-Q^2\hat{C}_{23}(0,0,Q^2;m_{H^0},0,0)\}\\
&\quad\times(2c/A^0):-h_{b_R}\{(d-2)\hat{C}_{24}(0,0,Q^2,m_{A^0},0,0)-Q^2\hat{C}_{23}(0,0,Q^2;m_{A^0},0,0)\}\\
&\quad\times(2d+2e/h^0):-2h_{b_L}\sin^2\alpha\ B_1(0;0,m_{h^0})\\
&\quad\times(2d+2e/H^0):-2h_{b_L}\cos^2\alpha\ B_1(0;0,m_{H^0})\\
&\quad\times(2d+2e/A^0):-2h_{b_L}B_1(0;0,m_{A^0})
\end{aligned} \tag{3.7}$$

with $Q^2=m_Z^2$. The charged-Higgs diagrams lead to corrections proportional to

$$\left(\frac{m_t\cot\beta}{m_W}\right)^2$$

and are suppressed compared to the neutral-Higgs diagrams by a factor of $(m_t/m_b\tan^2\beta)^2\sim(7.6/\tan\beta)^4$ so will be neglected. The shift in the left-handed coupling of the b to the Z is then

$$\delta h_{b_L}=\delta h_{b_L}^N+\delta h_{b_L}^C \tag{3.8}$$

with

$$\begin{aligned}
\delta h_{b_L}^N=&+\frac{g^2}{4}\left(\frac{m_b\tan\beta}{m_W}\right)^2\sin^2\alpha\{2\hat{C}_{24}(0,m_{h^0},m_{A^0})+\tfrac{1}{2}B_1(0,m_{h^0})+\tfrac{1}{2}B_1(0,m_{A^0})\}\\
&+\cos^2\alpha\{2\hat{C}_{24}(0,m_{H^0},m_{A^0})+\tfrac{1}{2}B_1(0,m_{H^0})+\tfrac{1}{2}B_1(0,m_{A^0})\}-h_{b_R}\sin^2\alpha\{(d-2)\hat{C}_{24}(m_{h^0},0,0)\\
&-m_Z^2\hat{C}_{23}(m_{h^0},0,0)+B_1(0,m_{h^0})\}-h_{b_R}\cos^2\alpha\{(d-2)\hat{C}_{24}(m_{H^0},0,0)-m_Z^2\hat{C}_{23}(m_{H^0},0,0)+B_1(0,m_{H^0})\}\\
&-h_{b_R}\{(d-2)\hat{C}_{24}(m_{A^0},0,0)-m_Z^2\hat{C}_{23}(m_{A^0},0,0,)+B_1(0,m_{A^0})\},\\
\delta h_{b_L}^C=&\,0.
\end{aligned} \tag{3.9}$$

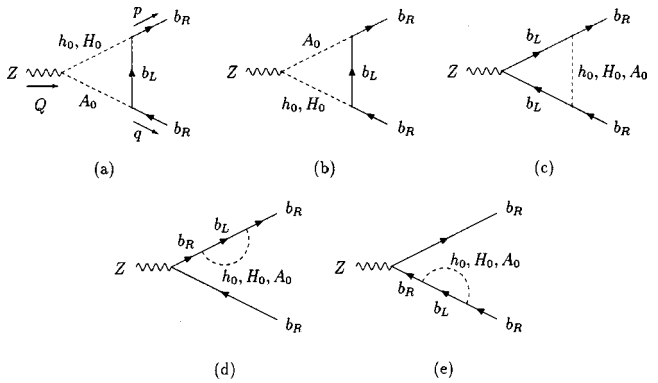

FIG. 2. One-loop neutral-Higgs corrections to $Z\to b_R\overline{b_R}$. Diagrams which correct $Z\to b_L\overline{b_L}$ can be obtained by the interchange $b_L\leftrightarrow b_R$.

Again, in the approximation $Q^2\to 0$, we find

$$\delta h^N_{b_L}\approx -\frac{1}{(4\pi)^2}\frac{g^2}{8}\left(\frac{m_b\tan\beta}{m_W}\right)^2\left[\sin^2\alpha\ G\left(\frac{m^2_{h^0}}{m^2_{A^0}}\right)+\cos^2\alpha\ G\left(\frac{m^2_{H^0}}{m^2_{A^0}}\right)\right]=-\delta h^N_{b_R}. \tag{3.10}$$

So in this approximation, the shift in the left-handed coupling of the b quark due to neutral-Higgs bosons is equal in magnitude but opposite in sign to the shift in the right-handed coupling.

To estimate the corrections to $Z\to u\overline{u}$, $c\overline{c}$, we note that the Higgs couplings to u and c quarks are suppressed either by $\tan\beta$ or by small d and s quark masses. Thus, we neglect these corrections.

The corrections to the τ couplings to the Z can be obtained from those of the b couplings by the simple substitutions

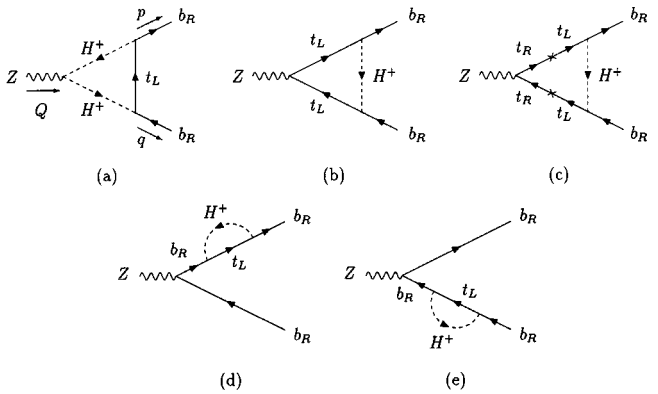

FIG. 3. One-loop charged-Higgs corrections to $Z\to b_R\overline{b_R}$. Diagrams which correct $Z\to b_L\overline{b_L}$ can be obtained by the substitution $b_R\to b_L, t_L\to t_R$.

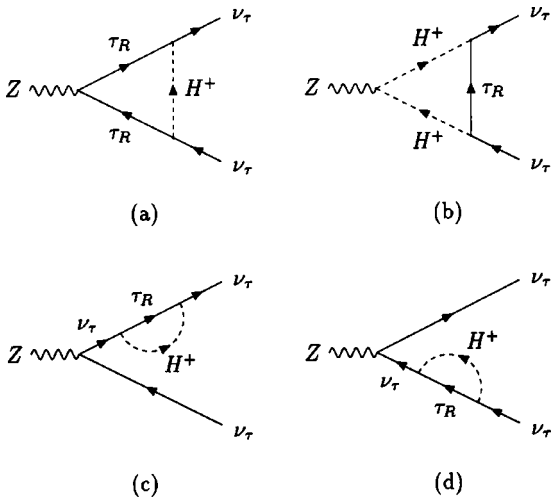

FIG. 4. Charged-Higgs corrections to $Z\to\nu_\tau\overline{\nu_\tau}$.

$$m_t, m_b\to 0, m_\tau,$$
$$h_{t_L}, h_{t_R}\to h_{\nu_L}, 0, \tag{3.11}$$
$$h_{b_L}, h_{b_R}\to h_{\tau_L}, h_{\tau_R}$$

which lead to

$$\delta h^N_{\tau_R}=-\delta h^N_{\tau_L}\approx+\frac{1}{(4\pi)^2}\frac{g^2}{8}\left(\frac{m_\tau\tan\beta}{m_W}\right)^2\left[\sin^2\alpha\ G\left(\frac{m^2_{h^0}}{m^2_{A^0}}\right)+\cos^2\alpha\ G\left(\frac{m^2_{H^0}}{m^2_{A^0}}\right)\right] \tag{3.12}$$
$$\delta h^C_{\tau_R}=\delta h^C_{\tau_L}=0.$$

Note that the charged-Higgs contribution is zero since m_t is replaced by $m_\nu=0$ and $F(m^2_\nu/m^2_{H^\pm})=F(0)=0$.

The decay $Z\to\nu_\tau\overline{\nu_\tau}$ is corrected by the diagrams shown in Fig. 4. The amplitude of these diagrams is

$$-\frac{g^2}{2}\left(\frac{m_\tau\tan\beta}{m_W}\right)^2\left[-i\frac{g}{\cos\theta_W}Z^\mu(Q)\overline{\nu}_{\tau L}(p)\gamma_\mu\nu_{\tau L}(q)\right]$$
$$\times(4a): h_{\tau_R}\{(d-2)\hat{C}_{24}(0,0,Q^2;m_{H^\pm},0,0)$$
$$-Q^2\hat{C}_{23}(0,0,Q^2;m_{H^\pm},0,0)\}$$
$$\times(4b): h_{H^+}2\hat{C}_{24}(0,0,Q^2;0,m_{H^\pm},m_{H^\pm})$$
$$\times(4c+4d): 2h_{\nu_L}B_1(0;0,m_{H^\pm}) \tag{3.13}$$

with $Q^2=m_Z^2$, resulting in a shift of the neutrino coupling by

$$\delta h^C_{\nu_L} = -\frac{g^2}{2}\left(\frac{m_\tau \tan\beta}{m_W}\right)^2 [h_{H^\pm}\{2\hat{C}_{24}(0,m_{H^\pm},m_{H^\pm}) + B_1(0,m_{H^\pm})\} + h_{\tau_R}\{(d-2)\hat{C}_{24}(m_{H^\pm},0,0) - m_Z^2\hat{C}_{23}(m_{H^\pm},0,0) + B_1(0,m_{H^\pm})\}]. \quad (3.14)$$

As a consequence of $F(0)=0$ we find

$$\delta h^C_{\nu_L} = 0. \quad (3.15)$$

To summarize, we have found that the nonzero shifts in the fermion couplings in our approximation ($Q^2=0$) are

$$\delta h^N_{b_R} = -\delta h^N_{b_L} = +\frac{1}{(4\pi)^2}\frac{g^2}{8}\left(\frac{m_b\tan\beta}{m_W}\right)^2\left[\sin^2\alpha\ G\left(\frac{m^2_{h^0}}{m^2_{A^0}}\right) + \cos^2\alpha\ G\left(\frac{m^2_{H^0}}{m^2_{A^0}}\right)\right],$$

$$\delta h^C_{b_R} = +\frac{1}{(4\pi)^2}\frac{g^2}{4}\left(\frac{m_b\tan\beta}{m_W}\right)^2 F\left(\frac{m_t^2}{m^2_{H^\pm}}\right), \quad (3.16)$$

$$\delta h^N_{\tau_R} = -\delta h^N_{\tau_L} = \left(\frac{m_\tau^2}{m_b^2}\right)\delta h^N_{b_R}.$$

Since $G(x)$ is negative semidefinite, the shifts in the left-handed couplings of the b and the τ due to the neutral-Higgs sector are both always *positive* while the shifts in the right-handed couplings are always *negative*, and they are all proportional to the same linear combination of G functions. Also, since $-1\leqslant F(x)\leqslant 0$, the charged-Higgs sector produces only a *negative* shift in h_{b_R} of magnitude at most

$$\frac{1}{(4\pi)^2}\frac{g^2}{4}\left(\frac{m_b\tan\beta}{m_W}\right)^2.$$

B. Fit to the data

We have identified the relevant vertex corrections to Z decay in the large tan β 2HDM. Using the LEP–SLD data to constrain their sizes will let us constrain the ratios

$$\frac{m^2_{h^0}}{m^2_{A^0}},\quad \frac{m^2_{H^0}}{m^2_{A^0}},\quad \text{and}\quad \frac{m_t^2}{m^2_{H^\pm}}.$$

All the neutral-Higgs corrections are proportional to each other, so we will use $\delta h^N_{\tau_L}$ as the fit parameter. For the charged-Higgs correction we will use $\delta h^C_{b_R}$.

In addition to the proper vertex corrections, the 2HDM corrects Z decay through oblique corrections which can be expressed as corrections to the ρ parameter and the effective value of $\sin^2\theta_W$. Since we will consider only ratios of partial widths and asymmetry parameters in our fit, the ρ parameter drops out from our analysis and we need only consider the shift in $\sin^2\theta_W$ which we will denote δs^2.[7] We will not utilize δs^2 to extract information on the 2HDM because oblique corrections are generically sensitive to other sorts of new physics as well.

The shifts to the $Zf\bar{f}$ couplings in the large tan β 2HDM can then be expressed as

$$\begin{aligned}
\delta h_{\nu_{eL}} &= \delta h_{\nu_{\mu L}} = \delta h_{\nu_{\tau L}} = 0,\\
\delta h_{e_{L,R}} &= \delta h_{\mu_{L,R}} = \delta s^2,\\
\delta h_{\tau_L} &= \delta s^2 + \delta h^N_{\tau_L},\\
\delta h_{\tau_R} &= \delta s^2 - \delta h^N_{\tau_L},\\
\delta h_{\mu_{L,R}} &= \delta h_{c_{L,R}} = -\tfrac{2}{3}\delta s^2,\\
\delta h_{d_{L,R}} &= \delta h_{s_{L,R}} = \tfrac{1}{3}\delta s^2,\\
\delta h_{b_L} &= \frac{1}{3}\delta s^2 + \left(\frac{m_b^2}{m_\tau^2}\right)\delta h^N_{\tau_L},\\
\delta h_{b_R} &= \frac{1}{3}\delta s^2 - \left(\frac{m_b^2}{m_\tau^2}\right)\delta h^N_{\tau_L} + \delta h^C_{b_R}.
\end{aligned} \quad (3.17)$$

The dependence of various observables on $\delta h^N_{b_R}$, $\delta h^C_{b_R}$, and δs^2 can be calculated in a straightforward manner. For example,

$$\frac{\delta A_e}{A_e} = \frac{4h_{e_L}h_{e_R}(h_{e_R}\delta h_{e_L} - h_{e_L}\delta h_{e_R})}{(h^4_{e_L} - h^4_{e_R})} = \frac{4h_{e_L}h_{e_R}(h_{e_R} - h_{e_L})}{h^4_{e_L} - h^4_{e_R}}\delta s^2 = -53.5\delta s^2,$$

where the coefficient has been calculated assuming $\sin^2\theta_W = 0.2315$. Similarly,

$$\frac{\delta A_\tau}{A_\tau} = -53.5\delta s^2 + 3.96\delta h^N_{\tau_L},$$

$$\frac{\delta A_{\rm FB}(e)}{A_{\rm FB}(e)} = \frac{\delta A_{\rm FB}(\mu)}{A_{\rm FB}(\mu)} = -107\delta s^2,$$

$$\frac{\delta A_{\rm FB}(\tau)}{A_{\rm FB}(\tau)} = -107\delta s^2 + 3.96\delta h^N_{\tau_L},$$

$$\frac{\delta R_e}{R_e} = \frac{\delta R_\mu}{R_\mu} = -0.84\delta s^2 - 2.89\delta h^N_{\tau_L} + 0.184\delta h^C_{b_R} + 0.307\delta\alpha_s,$$

[7] Similar techniques for isolating oblique corrections into one or just a few phenomenological parameters to extract constraints on proper vertex corrections were used in Refs. [13],[16–18].

TABLE I. LEP–SLD observables and their standard model predictions. The standard model predictions were calculated using ZFITTER v.6.21 [21] with $m_t = 174.3$ GeV [22], $m_H = 300$ GeV, and $\alpha_s(m_Z) = 0.120$ as input.

Observable	Reference	Measured value	ZFITTER prediction
		Z line-shape variables	
m_Z	[19]	91.1872 ± 0.0021 GeV	input
Γ_Z	[19]	2.4944 ± 0.0024 GeV	unused
$\sigma^0_{\rm had}$	[19]	41.544 ± 0.037 nb	unused
R_e	[19]	20.803 ± 0.049	20.739
R_μ	[19]	20.786 ± 0.033	20.739
R_τ	[19]	20.764 ± 0.045	20.786
$A_{\rm FB}(e)$	[19]	0.0145 ± 0.0024	0.0152
$A_{\rm FB}(\mu)$	[19]	0.0167 ± 0.0013	0.0152
$A_{\rm FB}(\tau)$	[19]	0.0188 ± 0.0017	0.0152
		τ polarization at LEP	
A_e	[19]	0.1483 ± 0.0051	0.1423
A_τ	[19]	0.1424 ± 0.0044	0.1424
		SLD left–right asymmetries	
$A_{\rm LR}$	[20]	$0.151\,08 \pm 0.002\,18$	0.1423
A_e	[20]	0.1558 ± 0.0064	0.1423
A_μ	[20]	0.137 ± 0.016	0.1424
A_τ	[20]	0.142 ± 0.016	0.1424
		Heavy quark flavor	
R_b	[19]	$0.216\,42 \pm 0.000\,73$	0.215 83
R_c	[19]	0.1674 ± 0.0038	0.1722
$A_{\rm FB}(b)$	[19]	0.0988 ± 0.0020	0.0997
$A_{\rm FB}(c)$	[19]	0.0692 ± 0.0037	0.0711
A_b	[19]	0.911 ± 0.025	0.934
A_c	[19]	0.630 ± 0.026	0.666

$$
\begin{aligned}
\frac{\delta R_\tau}{R_\tau} &= -0.84\,\delta s^2 + 5.07\,\delta h^N_{\tau_L} + 0.184\,\delta h^C_{b_R} + 0.307\,\delta\alpha_s\,,\\
\frac{\delta R_b}{R_b} &= 0.182\,\delta s^2 - 10.3\,\delta h^N_{\tau_L} + 0.652\,\delta h^C_{b_R}\,,\\
\frac{\delta R_c}{R_c} &= -0.351\,\delta s^2 + 2.89\,\delta h^N_{\tau_L} - 0.184\,\delta h^C_{b_R}\,,\\
\frac{\delta A_{\rm FB}(b)}{A_{\rm FB}(b)} &= -54.1\,\delta s^2 + 3.43\,\delta h^N_{\tau_L} - 1.73\,\delta h^C_{b_R}\,,\\
\frac{\delta A_{\rm FB}(c)}{A_{\rm FB}(c)} &= -58.7\,\delta s^2\,,\\
\frac{\delta A_b}{A_b} &= -0.681\,\delta s^2 + 3.43\,\delta h^N_{\tau_L} - 1.73\,\delta h^C_{b_R}\,,\\
\frac{\delta A_c}{A_c} &= -5.19\,\delta s^2
\end{aligned}
\tag{3.18}
$$

for $\sin^2\theta_W = 0.2315$, $\overline{m}_\tau(m_Z) = 1.777$ GeV, and $\overline{m}_b(m_Z) = 2.77$ GeV.[8] We have introduced the parameter $\delta\alpha_s$ to account for the deviation of $\alpha_s(m_Z)$ from its nominal value which we chose to be 0.120:[9]

$$\alpha_s(m_z) = 0.120 + \delta\alpha_s\,.$$

We fit the expressions in Eq. (3.18) to the differences between the LEP–SLD measurements and SM predictions shown in Table I. The corresponding correlation matrices of the data are given in Tables II and III. The SM predictions listed are for a SM Higgs boson mass of 300 GeV. Changing the SM Higgs boson mass has a negligible effect on all fit parameters except δs^2 which, as discussed above, we do not utilize except as a fit parameter.

The result of the fit was

$$
\begin{aligned}
\delta h^N_{\tau_L} &= -0.000\,21 \pm 0.000\,29,\\
\delta h^C_{b_R} &= 0.0049 \pm 0.0060,\\
\delta s^2 &= -0.000\,69 \pm 0.000\,19,\\
\delta\alpha_s &= -0.0007 \pm 0.0051
\end{aligned}
\tag{3.19}
$$

with the correlation matrix for the fit parameters shown in Table IV. The quality of the fit was $\chi^2 = 18.4/(18-4)$. The largest contributions to the χ^2 come from $A_{\rm FB}(b)$ (3.5) and $A_{\rm LR}$ (2.5) which means that the 2HDM corrections do not improve the agreement between the theoretical and experimental values of these observables.

In Figs. 5–7 we show how different observables constrain the parameters $\delta h^N_{\tau_L}$, $\delta h^C_{b_R}$, and δs^2. Since $\delta h^N_{\tau_L}$ is the only parameter which breaks lepton universality, it is most strongly constrained by the ratios R_l $(l = e, \mu, \tau)$. This is evident from Figs. 5 and 6. This places a tight constraint on the size of the neutral-Higgs correction to the b quark observables.[10] The charged-Higgs contribution, $\delta h^C_{b_R}$, must then fit all the heavy flavor observables, but due to the small experimental error on R_b, it is also constrained to be small. In Fig. 7, one sees that the overlap of the $A_{\rm LR}$ and $A_{\rm FB}(b)$ bands prefers a value of δh_{b_R} of about 0.04, far from the SM point at the origin.[11] However, the R_b band does not allow this deviation, leading to the large χ^2's for $A_{\rm LR}$ and $A_{\rm FB}(b)$ mentioned above. Note also that the large tan β 2HDM predicts $\delta h^C_{b_R} \leqslant 0$ so it cannot account for the ''A_b anomaly'' even if the constraint from R_b were absent. In fact, since the

[8] Letting $\overline{m}_b(m_Z)$ change by 10% in either direction will only change the final central value of $\delta h^N_{\tau_L}$ by about a fifth of a σ.

[9] The value of $\alpha_s(m_Z)$ from LEP is determined by fitting the SM to R_l, $(l = e, \mu, \tau)$. Since we are considering extra corrections to the R_l's, we must let $\alpha_s(m_Z)$ float in our fit.

[10] This was pointed out by Hisano *et al.* in Ref. [7].

[11] This is the ''A_b anomaly'' mentioned in the Introduction. See, for instance, Refs. [10] and [11].

TABLE II. The correlation of the Z line-shape variables at LEP.

	m_Z	Γ_Z	$\sigma^0_{\rm had}$	R_e	R_μ	R_τ	$A_{\rm FB}(e)$	$A_{\rm FB}(\mu)$	$A_{\rm FB}(\tau)$
m_Z	1.000	−0.008	−0.050	0.073	0.001	0.002	−0.015	0.046	0.034
Γ_Z		1.000	−0.284	−0.006	0.008	0.000	−0.002	0.002	−0.003
$\sigma^0_{\rm had}$			1.000	0.109	0.137	0.100	0.008	0.001	0.007
R_e				1.000	0.070	0.044	−0.356	0.023	0.016
R_μ					1.000	0.072	0.005	0.006	0.004
R_τ						1.000	0.003	−0.003	0.010
$A_{\rm FB}(e)$							1.000	−0.026	−0.020
$A_{\rm FB}(\mu)$								1.000	0.045
$A_{\rm FB}(\tau)$									1.000

best fit value of $\delta h^C_{b_R}$ is still small but positive, the 2HDM is slightly disfavored by the data.

The same can be said of $\delta h^N_{\tau_L}$: Since the experimental value of R_τ is smaller than those for R_μ and R_e, it is easy to see from Eq. (3.18) that the data prefer a negative value of $\delta h^N_{\tau_L}$. However, the large tan β 2HDM predicts $\delta h^N_{\tau_L} \geqslant 0$.

C. Constraints on model parameters

Since $\delta h^N_{\tau_L} \geqslant 0$ and $\delta h^C_{b_R} \leqslant 0$ for the large tan β 2HDM in our approximation, the best fit values of $\delta h^N_{\tau_L}$ and $\delta h^C_{b_R}$ consistent with the model are $\delta h^N_{\tau_L} = \delta h^C_{b_R} = 0$, corresponding to the standard model case. Thus, the large tan β 2HDM does not mitigate the A_b problem, nor does it even improve agreement between the theoretical predictions for R_b and R_τ and the experimental data.[12]

In order to extract the limits on the Higgs mass ratios from Eq. (3.19), we have performed both classical and Bayesian statistical analyses, in the latter assuming a uniform prior probability for the parameter regions $\delta h^N_{\tau_L} \geqslant 0$ and

$$0 \geqslant \delta h^C_{b_R} \geqslant -\frac{1}{(4\pi)^2}\frac{g^2}{4}\left(\frac{m_b \tan\beta}{m_W}\right)^2. \tag{3.20}$$

[Recall that

$$\delta h^C_{b_R} = \frac{1}{(4\pi)^2}\frac{g^2}{4}\left(\frac{m_b \tan\beta}{m_W}\right)^2 F\left(\frac{m_t^2}{m^2_{H^\pm}}\right)$$

and $-1 \leqslant F(x) \leqslant 0$.]

The corresponding {68%} and [95%] confidence limits on the fit parameters are

$$\begin{aligned} \text{classical:}\quad & \delta h^C_{b_R} \geqslant \{-0.0011\}[-0.0071], \\ & \delta h^N_{\tau_L} \leqslant \{0.000\,08\}[0.000\,37], \\ \text{Bayesian:}\quad & \delta h^C_{b_R} \geqslant \{-0.0021\}[-0.0050], \\ & \delta h^N_{\tau_L} \leqslant \{0.000\,11\}[0.000\,25]. \end{aligned} \tag{3.21}$$

Using $2m_W/g = 246$ GeV and $\overline{m}_b(m_Z) = 2.77$ GeV, the bounds on $\delta h^C_{b_R}$ translate into the bounds on $F(x)$, where $x = m_t^2/m^2_{H^\pm}$:

$$\begin{aligned} \text{classical:}\quad & F(x) \geqslant \left\{-\left(\frac{37}{\tan\beta}\right)^2\right\}\left[-\left(\frac{94}{\tan\beta}\right)^2\right], \\ \text{Bayesian:}\quad & F(x) \geqslant \left\{-\left(\frac{52}{\tan\beta}\right)^2\right\}\left[-\left(\frac{79}{\tan\beta}\right)^2\right]. \end{aligned} \tag{3.22}$$

For tan $\beta < 94$, the entire range of $F(x)$ is contained in the classical 95% confidence region [since $-1 \leqslant F(x) \leqslant 0$]. It is

[12] Similar behavior in the context of the MSSM with R-parity violation was observed in Ref. [16]. There, the preferred values of the fit parameters were again the opposite sign of what the model predicted, and moreover, more than one to two σ away from zero. This was a manifestation of the A_b anomaly. In the model considered here, the A_b anomaly is not as manifest in the fit results, since there are fewer new physics parameters.

TABLE III. The correlation of the heavy flavor variables from LEP–SLD.

	R_b	R_c	$A_{\rm FB}(b)$	$A_{\rm FB}(c)$	A_b	A_c
R_b	1.00	−0.14	−0.03	0.01	−0.03	0.02
R_c		1.00	0.05	−0.05	0.02	−0.02
$A_{\rm FB}(b)$			1.00	0.09	0.02	0.00
$A_{\rm FB}(c)$				1.00	−0.01	0.03
A_b					1.00	0.15
A_c						1.00

TABLE IV. The correlation matrix of the fit parameters.

	$\delta h^N_{\tau_L}$	$\delta h^C_{b_R}$	δs^2	$\delta\alpha_s$
$\delta h^N_{\tau_L}$	1.00	0.62	−0.12	−0.30
$\delta h^C_{b_R}$		1.00	−0.22	−0.63
δs^2			1.00	0.25
$\delta\alpha_s$				1.00

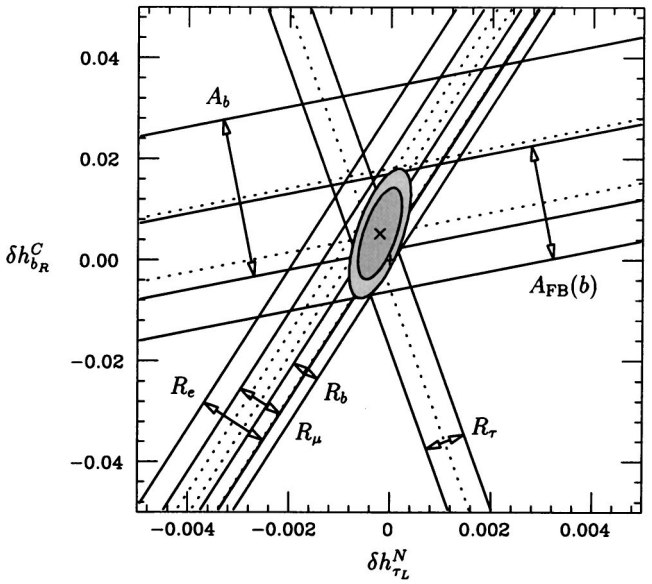

FIG. 5. The 1σ constraints on $\delta h^N_{\tau_L}$ and $\delta h^C_{b_R}$ from various observables in the $\delta s^2=\delta\alpha_s=0$ plane. The shaded contours represent the 68% and 90% confidence limits.

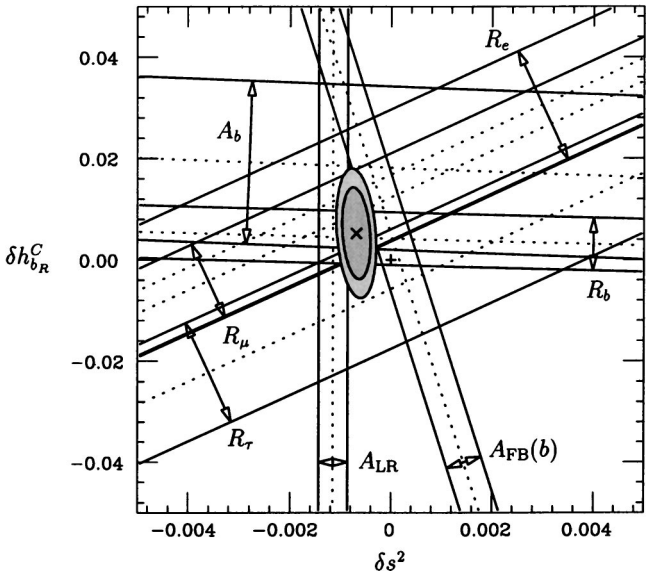

FIG. 7. The 1σ constraints on $\delta h^C_{b_R}$ and δs^2 from various observables in the $\delta h^N_{\tau_L}=\delta\alpha_s=0$ plane. The shaded contours represent the 68% and 90% confidence limits.

therefore difficult to significantly bound the charged-Higgs mass using this method unless $\tan\beta$ is quite large. Choosing $\tan\beta=100$ for definiteness, we translate the bounds on $F(x)$ into bounds on $m_{H^\pm}$:

$$\begin{aligned} &\text{classical:} \quad m_{H^\pm}\geqslant\{670\ \text{GeV}\}\ [40\ \text{GeV}],\\ &\text{Bayesian:} \quad m_{H^\pm}\geqslant\{370\ \text{GeV}\}\ [120\ \text{GeV}], \end{aligned} \tag{3.23}$$

Bounds on $m_{H^\pm}$ are plotted as a function of $\tan\beta$ in Fig. 8.

Bounds on the neutral-Higgs sector masses from constraints on $\delta h^N_{\tau_L}$ are more model dependent than charged-Higgs bounds, since $\delta h^N_{\tau_L}$ involves the masses of all of the neutral Higgs bosons and the mixing angle α. Generally, requiring the magnitude of $\delta h^N_{\tau_L}$ to be small constrains the scalar–pseudoscalar mass splittings to be small. To give a concrete example (as in Refs. [7],[9]), let us consider the limit $\alpha=\beta\approx\pi/2$,

$$\delta h^N_{\tau_L}=-\frac{1}{(4\pi)^2}\frac{g^2}{8}\left(\frac{m_\tau\tan\beta}{m_W}\right)^2 G\left(\frac{m^2_{h^0}}{m^2_{A^0}}\right). \tag{3.24}$$

In this approximation the {68%} and [95%] lower limits on $G(m^2_{h^0}/m^2_{A^0})$ (which is negative semidefinite) are

$$\text{classical:} \quad G\left(\frac{m^2_{h^0}}{m^2_{A^0}}\right)\geqslant\left\{-\left(\frac{22}{\tan\beta}\right)^2\right\}\left[-\left(\frac{47}{\tan\beta}\right)^2\right], \tag{3.25}$$

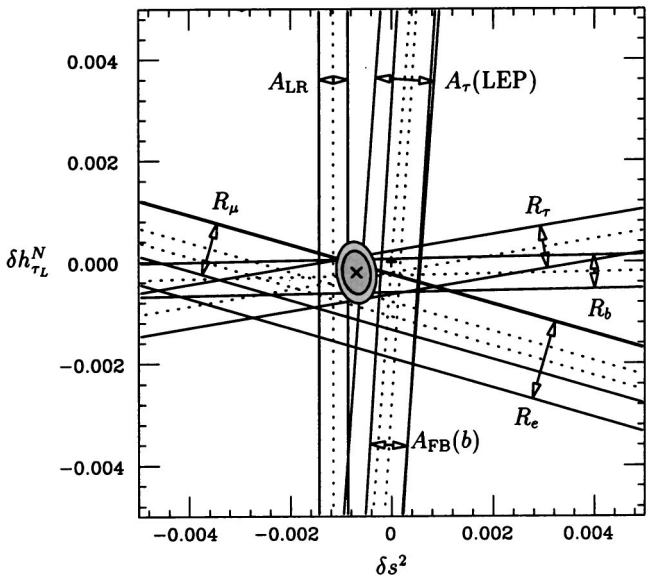

FIG. 6. The 1σ constraints on $\delta h^N_{\tau_L}$ and δs^2 from various observables in the $\delta h^C_{b_R}=\delta\alpha_s=0$ plane. The shaded contours represent the 68% and 90% confidence limits.

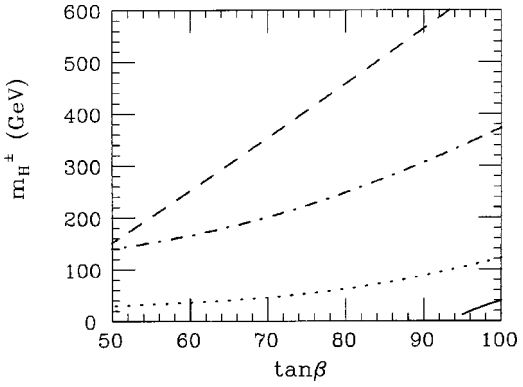

FIG. 8. Lower bounds on the charged-Higgs mass vs $\tan\beta$. The dotted–dashed and dotted lines correspond to the Bayesian 68% and 95% confidence levels, respectively. The dashed and solid lines correspond to the classical 68% and 95% confidence levels, respectively.

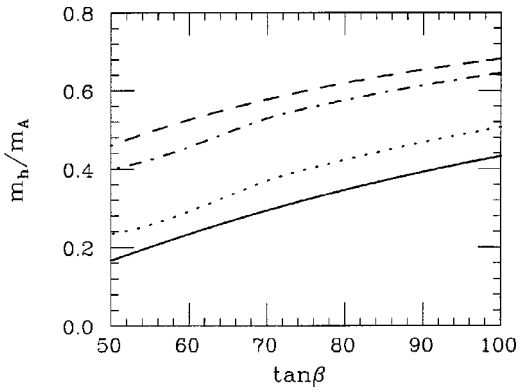

FIG. 9. Lower bounds on the scalar–pseudoscalar mass ratio vs tan β. The dotted–dashed and dotted lines correspond to the Bayesian 68% and 95% confidence levels, respectively. The dashed and solid lines correspond to the classical 68% and 95% confidence levels, respectively.

$$\text{Bayesian:}\quad G\left(\frac{m_{h^0}^2}{m_{A^0}^2}\right)\geqslant\left\{-\left(\frac{25}{\tan\beta}\right)^2\right\}\left[-\left(\frac{39}{\tan\beta}\right)^2\right].$$

With the choice $\tan\beta=100$ we find that our bounds on G translate into bounds on the h^0-A^0 mass splitting (choosing the branch of solutions with $m_{h^0}/m_{A^0}<1$):

$$\begin{aligned}&\text{classical:}\quad 1\geqslant\frac{m_{h^0}}{m_{A^0}}\geqslant\{0.68\}[0.43],\\ &\text{Bayesian:}\quad 1\geqslant\frac{m_{h^0}}{m_{A^0}}\geqslant\{0.64\}[0.51].\end{aligned}\tag{3.26}$$

More generally, bounds on m_{h^0}/m_{A^0} are plotted as a function of $\tan\beta$ in Fig. 9. In the limit $\sin\alpha\sim 0$, the result is the same, except that m_{H^0}/m_{A^0} replaces m_{h^0}/m_{A^0} in the above expressions.

IV. SUMMARY AND CONCLUSIONS

We have analyzed the implications of the large $\tan\beta$ 2HDM for Z decays and for lepton universality violation in W decays. For Z decays we find that the generic predictions of the model do not improve agreement between theory and experiment. Further, the LEP–SLD experimental uncertainty in the measurement of lepton universality is sufficiently small to place significant constraints on mass splittings in the neutral-Higgs sector for large $\tan\beta$. Constraints from the b decay parameters are sufficient to place bounds on the charged-Higgs mass that are increasingly strong for increasing $\tan\beta$. For instance, for $\tan\beta=100$ we obtain the 1σ classical (Bayesian) bounds of

$$m_{H^\pm}\geqslant 670\ \text{GeV}\ \ (370\ \text{GeV})$$

and

$$1\geqslant\left.\frac{m_{h^0}}{m_{A^0}}\right|_{\alpha=\beta}=\left.\frac{m_{H^0}}{m_{A^0}}\right|_{\alpha=0}\geqslant 0.68\ \ (0.64).\tag{4.1}$$

For W decays, the experimental central value from DØ slightly disfavors the generic prediction of the model, but experimental uncertainties are too large to usefully constrain the charged–neutral-Higgs mass splittings.

ACKNOWLEDGMENTS

This work was supported in part (O.L. and W.L.) by the U.S. Department of Energy, Grant No. DE-FG05-92-ER40709, Task A.

APPENDIX: FEYNMAN INTEGRALS

The integrals we use here are defined explicitly in [13]. In the approximation $p^2=0$, the one-loop diagrams which appear in this work are proportional to the following expressions:

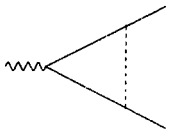

$$\begin{aligned}&\propto[(d-2)\hat{C}_{24}(0,0,p^2;m_s,m_f,m_f)-m_Z^2\hat{C}_{23}(0,0,p^2;m_s,m_f,m_f)]\\ &\approx-\frac{1}{(4\pi)^2}\left[\frac{1}{2}\left(\Delta_\epsilon-\ln\frac{m_f^2}{\mu^2}\right)+f(x)\right],\end{aligned}\tag{A1}$$

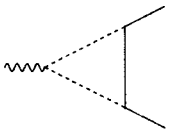

$$\propto 2\hat{C}_{24}(0,0,p^2;m_f,m_s,m_s)\approx-\frac{1}{(4\pi)^2}\left[\frac{1}{2}\left(\Delta_\epsilon-\ln\frac{m_f^2}{\mu^2}\right)-g(x)\right]\tag{A2}$$

or

$$\propto 2\hat{C}_{24}(0,0,p^2;0,m_{s_1},m_{s_2})\approx-\frac{1}{2(4\pi)^2}\left[\Delta_\epsilon+\frac{3}{2}-\frac{m_{s_1}^2\ln m_{s_1}^2-m_{s_2}^2\ln m_{s_2}^2}{m_{s_1}^2-m_{s_2}^2}\right],\tag{A3}$$

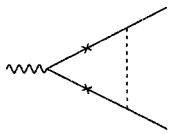

$$\propto m_f^2 \hat{C}_0(0,0,p^2;m_s,m_f,m_f) \approx -\frac{1}{(4\pi)^2}[f(x)+g(x)], \tag{A4}$$

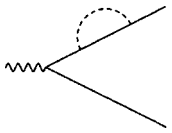

$$\propto \hat{B}_1(0;m_f,m_s) \approx \frac{1}{(4\pi)^2}\left[\frac{1}{2}\left(\Delta_\epsilon - \ln\frac{m_f^2}{\mu^2}\right) - g(x)\right], \tag{A5}$$

where

$$f(x) = -\frac{1}{4(1-x)^2}(x^2-1-2\ln x), \quad g(x) = -\frac{1}{2}\ln x + \frac{1}{4(1-x)^2}[-(1-x)(1-3x)+2x^2\ln x] \tag{A6}$$

for $x = m_f^2/m_s^2$. Note that the function $F(x)$ appearing in Eq. (3.6) is defined as

$$F(x) = f(x) + g(x).$$

For $x \to 1$ (degenerate scalar and fermion masses),

$$f(x) \approx -\frac{1}{2} + \frac{x-1}{6} + \cdots, \quad g(x) \approx -\frac{x-1}{3} + \cdots. \tag{A7}$$

For $x \to 0$ (the decoupling limit of heavy scalar masses),

$$f(x) \approx \tfrac{1}{2}\ln x + \tfrac{1}{4} + \cdots, \quad g(x) \approx -\tfrac{1}{2}\ln x - \tfrac{1}{4} + \cdots \sim -f(x). \tag{A8}$$

The function $G(x)$ defined in Eq. (2.6) is symmetric under $x \leftrightarrow 1/x$. For $x \to 0, \infty$,

$$G(x) \sim -\left|\frac{\ln x}{2}\right| + 1 + \cdots. \tag{A9}$$

For $x \to 1$ (the decoupling limit of degenerate scalar masses),

$$G(x) \sim -\tfrac{1}{12}(x-1)^2 + \cdots. \tag{A10}$$

[1] For a recent review, see H. E. Haber, in *Perspectives on Higgs Physics II*, edited by G. L. Kane (World Scientific, Singapore, 1997), hep-ph/9707213.

[2] See, for example, W. Loinaz and J. D. Wells, Phys. Lett. B **445**, 178 (1998).

[3] F. M. Borzumati and C. Greub, Phys. Rev. D **58**, 074004 (1998).

[4] M. Ciuchini, G. Degrassi, P. Gambino, and G. F. Giudice, Nucl. Phys. **B527**, 21 (1998).

[5] A. Denner, R. J. Guth, W. Hollik, and J. H. Kuhn, Z. Phys. C **51**, 695 (1991).

[6] A. K. Grant, Phys. Rev. D **51**, 207 (1995).

[7] J. Hisano, S. Kiyoura, and H. Murayama, Phys. Lett. B **399**, 156 (1997).

[8] H. E. Logan, hep-ph/9906332.

[9] H. E. Haber and H. E. Logan, Phys. Rev. D **62**, 015011 (2000).

[10] M. S Chanowitz, hep-ph/9905478.

[11] J. H. Field and D. Sciarrino, hep-ex/9907018.

[12] J. F. Gunion, H. E. Haber, G. L. Kane, and S. Dawson, *The Higgs Hunter's Guide* (Addison-Wesley, Redwood City, CA, 1989).

[13] O. Lebedev, W. Loinaz, and T. Takeuchi, Phys. Rev. D **61**, 115005 (2000).

[14] CDF and DØ collaborations, F. Rimondi, presented at 13th Topical Conference on Hadron Collider Physics, Mumbai, India, 1999, FERMILAB-CONF-99-063-E.

[15] P. H. Chankowski, M. Krawczyk, and J. Zochowski, Eur. Phys. J. C **11**, 661 (1999).

[16] O. Lebedev, W. Loinaz, and T. Takeuchi, Phys. Rev. D **62**, 015003 (2000).

[17] W. Loinaz and T. Takeuchi, Phys. Rev. D **60**, 015005 (1999).

[18] T. Takeuchi, A. K. Grant, and J. L. Rosner, in *The Proceedings of DPF'94*, Albuquerque, NM, 1994, edited by S. Seidel (World Scientific, Singapore, 1995), hep-ph/9409211.

[19] J. Mnich, CERN-EP/99-143; M. Swartz, talk presented at Lepton–Photon'99, Stanford, 1999 (transparencies available from http://www-sldnt.slac.stanford.edu/lp99/); S. Fahey and G. Quast, talks presented at EPS–HEP'99, Tampere, Finland, 1999, (transparencies available from http://neutrino.pc.helsinki.fi/hep99/).

[20] SLD collaboration, K. Abe *et al.*, hep-ex/9908006; The SLD collaboration, J. E. Brau, talk presented at EPS–HEP'99, Tam-

pere, Finland, 15 July 1999 (transparencies available from http://www-sld.slac.stanford.edu/sldwww/pubs.html).

[21] The ZFITTER package, D. Bardin *et al.*, Z. Phys. C **44**, 493 (1989); Nucl. Phys. **B351**, 1 (1991); Phys. Lett. B **255**, 290 (1991); CERN-TH-6443/92, 1992; DESY 99-070, hep-ph/9908433.

[22] The Top Averaging Group, L. Demortier *et al.*, FERMILAB-TM-2084.